

## Title

Optic flow stabilizes flight in ruby-throated hummingbirds

## Authors

Ivo G. Ros<sup>1\*</sup>, Andrew A. Biewener<sup>2</sup>

**Author affiliation.** <sup>1,2</sup>Harvard University, Department of Organismic and Evolutionary Biology, Concord Field Station, 100 Old Causeway Road, Bedford, MA 01730, USA

<sup>1</sup>Current address: California Institute of Technology, Division of Biology and Biological Engineering, Pasadena, CA 91125, USA

\*Ivo.Ros@gmail.com

## Keywords

Optic flow; Flight control; Hummingbird; Visuomotor delay

## Summary

Flying birds rely on visual cues for retinal image stabilization by negating rotation-induced optic flow, the motion of the visual panorama across the retina, through corrective eye and head movements. In combination with vestibular and proprioceptive feedback, birds may also use visual cues to stabilize their body during flight. Here, we test whether artificially induced wide-field motion generated through projected visual patterns elicits maneuvers in body orientation and flight position, in addition to stabilizing vision. To test this hypothesis, we present hummingbirds flying freely within a 1.2 m cylindrical visual arena with a virtual surround rotated at different speeds about its vertical axis. The birds responded robustly to these visual perturbations by rotating their heads and bodies with the moving visual surround, and by adjusting their flight trajectories; following the surround. Thus, similar to insects, hummingbirds appear to use optic flow cues to control flight maneuvers in addition to stabilize their visual inputs.

## Introduction

Flight control is crucial to ecologically relevant behaviors such as predator-prey interactions, courtship, and foraging in dynamically and geometrically complex environments (Dudley, 2002). Flight stability, the ability to resist and recover from perturbations, and flight maneuverability, the ability to change orientation and position (Guckenheimer and Holmes 1983, Sefati et al. 2013; Dudley, 2002) are fundamental components of flight control. To actively stabilize flight by means of compensatory motor commands against external perturbations, such as turbulent air or wind gusts, detection of self-motion is required as a control-input. Birds fly in complex three-dimensional environments and can detect self-motion using their visual, vestibular and proprioceptive systems (Warren & Wertheim, 1990). Additionally, filoplume-associated mechano-receptors can sense air flow (Gewecke and Woike, 1978). In cases of conflicting signals, evidence exists that the visual system overrules other sensory modalities for retinal image stabilization (Friedman, 1975, Gioanni, 1988). An important visual cue that indicates self-motion is optic flow: the resulting movement of the panorama, or visual surround, across the retinae (Gibson, 1958; Koenderink, 1986; Koenderink and Van Doorn, 1987). Optic flow arises from self-motion, whether voluntarily generated by the animal's motion or resulting from a perturbation, such as a wind gust during flight.

A variety of animals ranging from vertebrates to arthropods reduce rotation-induced optic flow by means of eye, head and/or body rotations (Walls, 1962; Reviews in insects: Reichardt 1969; Egelhaaf *et al.* 1988). These optomotor responses thereby stabilize the retinal image, facilitating the extraction of translational self-motion and depth information (Egelhaaf *et al.*, 2012), and improving image resolution (Westheimer and McKee, 1975), as well as the ability to detect object motion (Nakayama, 1975).

It is known that birds use optic flow to guide various sensorimotor behaviors. Budgerigars choose flight paths that balance optic flow between the left and right sides, and regulate flight speed using cues based on optic flow, similar to insects (Bhagavatula *et al.*, 2011; Schiffner & Srinivasan, 2015; Baird *et al.*, 2005; Fry *et al.*, 2009). Optic flow parameters, such as *tau* representing time-to-contact, are also used by hawks and pigeons to land (Davies & Green, 1990) and by hummingbirds to approach feeders (Lee *et al.*, 1993 & 1991). Recently,

hummingbirds have also been shown to control hovering position using optic flow (Goller & Altshuler, 2014).

Additionally, certain wing and tail muscles in pigeons respond to head deflections induced by rotational visual stimulation during simulated flight (Bilo, 1992), indicating that optic flow is involved in rotational flight stabilization, as demonstrated in insects (*e.g.* Collet & Land, 1975; Lehrer & Srinivasan, 1992; Farina *et al.* 1995; Kern & Varju, 1998; Mronz & Lehmann, 2008; Theobald *et al.*, 2009; Windsor *et al.*, 2014), and suggested in hummingbirds and zebra finches (Srinivasan, 2001; Iwaniuk & Wylie, 2007; Eckmeier *et al.*, 2013).

During locomotion, the optomotor response mostly separates the two components of optic flow that result from the bird's *i*) translational motion as it moves from one place to another, and *ii*) rotational motion as it changes from one orientation to another (Egelhaaf *et al.* 2012; Eckmeier *et al.*, 2008). Flight control requires both optic flow components because translational optic flow contains course, speed and depth information, while rotational optic flow informs a bird about its own rotations (Egelhaaf *et al.*, 2012). Both translational and rotational components of optic flow are encoded in nuclei within the accessory optic system (AOS) of the avian visual system (Wylie & Frost, 1990).

Among birds, hummingbirds have an enlarged nucleus lentiformis mesencephali, one of the nuclei within the AOS involved in optic flow processing. Because of this neural specialization, combined with their stellar hovering and precision flight capabilities, hummingbirds are ideal species to test for a role of optic flow in avian flight stabilization (Iwaniuk & Wylie, 2007; Srinivasan, 2001; Greenewalt, 1960).

Here, we address whether hummingbirds use optic flow under free-flight conditions to control body orientation and flight position, in addition to stabilizing their vision. We present wide-field motion to free-flying hummingbirds in the form of rotations of their full 360° panorama by means of projecting moving images on a cylindrical surround (Fig. 1A-B; Video S1). We test whether these visual perturbations elicit corrective responses in horizontal body rotations and flight paths. In general, wide-field motion should not evoke a robust and well-matched compensatory flight response, if the visual surround is only used to stabilize vision. To solely stabilize vision, we would expect optokinetic head nystagmus without, or possibly with sporadic, optokinetic control of flight position or body orientation in the horizontal plane. In

other words, we would expect that hummingbirds would only visually track their surround with smooth head rotations (until a fast head rotation returns the head to its original orientation), but without corresponding body rotations or changes in flight path (Gioanni, 1988). However, if the visual surround is also used to control body orientation and flight position, wide field image motion should elicit corrective maneuvers during flight. We therefore hypothesize that hummingbirds perform horizontal body rotations and changes in flight position, in addition to making smooth head rotations. We expect these corrective maneuvers to reduce rotational and translational optic flow imposed by the rotating surround, indicating the importance of optic flow for flight control, as well as stabilization of the visual input.

## Materials and Methods

Five female ruby-throated hummingbirds, *Archilocus colubris*, were trapped in Bedford, Massachusetts, USA, and studied in accordance with protocols approved by Harvard University's Institutional Animal Care and Use Committee.

To generate a visual stimulus of surround rotations, four projectors (BenQ MW663) were distributed around a 1.2 m inner diameter, vertically oriented acrylic cylinder. The cylinder was coated for rear-projection, extraneous visual cues were eliminated with black fabric, and an acrylic ceiling two-thirds of the cylinder height supported a syringe with artificial nectar. Thirty-two equal-width vertical bars (alternating black and white) were projected synchronously at 120 frames per second, with the image displacement between projection frames determining the rotation speed.

Given the short photoreceptor response time expected of hummingbirds (Healy *et al.*, 2013), we projected under low-light conditions to lower their critical fusion frequency. The projected images resulted in an illuminance of 38 lux at the center, and a Michelson contrast of 0.8 at the perimeter of the cylinder. The surround was either held stationary or rotated horizontally in either direction at 62, 98 or 134° s<sup>-1</sup>, resulting in seven experimental conditions. Quantified movements and directions were expressed relative to stimulus direction, with positive values indicating the bird's movement with the surround.

Observed from the cylinder center, the spatial frequency of 0.04 cycles per degree combined with the rotation speeds (62, 98, and 134° s<sup>-1</sup>) corresponds to temporal frequencies of

2.8, 4.4 and 6.0 Hz, which are within the range of the broadly tuned, fast directional neurons in the avian pretectum (Ibbotson, 2001; *e.g.*  $(16 \text{ cycles} / 360^\circ) \times 134^\circ \text{ s}^{-1} = 6 \text{ Hz}$  (Fig 1A)). Under these free-flight conditions the specific perceived frequencies vary depending on the bird's position within the cylinder and its perceptual focus. However, for the test here of a link between wide-field motion and control of body orientation and flight position, the specific spatial and temporal frequencies experienced by the bird are not critical, provided the frequencies remain within the range of the avian pretectum. The square-wave grating was kept constant and of a sufficiently low spatial frequency to avoid aliasing effects causing potential directional ambiguity at higher rotation speeds.

The hummingbirds flew freely within the cylinder and were recorded with two Photron 1024 PCI cameras at 500 Hz (Fig. 1A), for which sufficient illumination was provided by two 850 nm wavelength infra-red LED arrays that were imperceptible to the hummingbirds.

Using thermoplastic and cyanoacrylate adhesives, four white, 2-3 mm diameter, polystyrene markers were attached to each individual: on the head, two markers were positioned near the lateral ends of the coronal suture of the skull, and on the body, two markers were positioned dorsally over the spine, separated by 14 mm (Fig. 1B). Additionally, a 2 mm diameter dot of white non-toxic correction fluid was deposited on the bill. The maximum mass added to a bird was 0.04 g (1% body mass).

Using the two calibrated high-speed camera views, 3D positions of the markers were reconstructed in Matlab (Hedrick, 2008) within a  $0.2 \text{ m}^3$  volume at the center of the cylinder, resulting in a spatial measuring error of less than 0.4 mm. The orientation in the horizontal plane of the marker-based direction-vector was calculated for both head and body, with the time-derivative giving the rotational velocity (Figs. 2; 3A-C). For the current study 'orientation' refers to the horizontal component of orientation, which is more commonly used for 3D angular position. Both head and body orientation were referenced to the body orientation at time = 0 s (start of surround rotation or start of stationary recordings). Therefore, the difference between the reported head and body angles represented the body-head offset throughout. Concentric flight velocity, *i.e.* the component of the flight velocity parallel to the nearest wall tangent, was based on a virtual head center marker (Fig. 1B, inset), with the time-integral from the start of a recording giving the concentric flight distance (Fig. 1C-E).

Statistics were performed in JMP (SAS Institute), with the multiple least-squares linear regressions models corrected for individual effects (Fig. 3B-D).

## Results

Hummingbirds, hovering freely within a large vertical cylinder, were presented with a rotating visual panorama, or surround (Fig. 1A-B; Video S1). The surround, which was comprised of thirty-two alternating black and white, vertical bars, was projected from the outside on a 1.2 m diameter cylinder at 120 frames per second that covered the full 360° panorama. This surround was either held stationary or rotated at 62, 98 or 134° s<sup>-1</sup> in left or right directions, resulting in seven stimulus conditions. Synchronized high speed camera views combined with markers on the birds allowed us to quantify the behavioral response in terms of horizontal head and body rotations and the component of flight speed parallel to the wall (concentric flight speed) (Fig. 1B, inset). To compare the hummingbird's behavioral responses to rotating surrounds with its flight behavior with a stationary surround, each stimulation condition was initiated remotely by the researcher without knowledge of the bird's position within the cylinder, with the bird's response tracked for a period between 0.8 s and 1.8 s.

The five hummingbirds hovered with a wingbeat frequency of  $42.7 \pm 1.3$  Hz. During trials in a stationary surround, voluntary fast head rotations, or head saccades, alternated with periods of no perceivable head rotation (stabilization; Fig. 1C). During trials with a rotating surround ( $\pm 62, 98$  and  $134^\circ \text{ s}^{-1}$ ), the hummingbirds displayed classic optokinetic head nystagmus, where fast head saccades alternated with slow phases of head rotations (Fig. 1D, E; see Giovanni and Sansonetti, 1999). During the slow phases, the head always rotated in the same direction as the surround (Fig. 1C-E; Fig. 2). Furthermore, after approximately 0.5 s following stimulus onset (first observed displacement of the surround), the speed of the slow phases leveled off and closely matched that of the surround (Fig. 3A). To perform balanced comparisons of the behavioral responses across trials and individuals, we selected a 1 s period for all trials. Between 0.5 to 1.5 s after stimulus onset, head rotation velocity correlated with the surround speed (adjusted  $R^2 = 0.98$ ,  $p < 0.001$ ; multiple least-squares linear regressions model, which included the trends of individual birds as random effects, in order to correct for individual differences for all regressions; Fig. 3B).

For 81 head saccades observed in the 5 individuals,  $75\% \pm 18\%$  (mean  $\pm$  SD) of these fast head rotations turned with the direction of the projected surround and  $25\% \pm 18\%$  of the cases against (*e.g.* Fig. 1E; two-sample t-test  $p < 0.05$ ).

Body rotations were more continuous, but generally followed head rotations (Fig. 1C-E). Surround speed during the period 0.5 to 1.5 s after stimulus onset predicted body rotation velocity (adjusted  $R^2 = 0.17$ ;  $p < 0.001$ ; Fig. 3C), though not as strongly as the slow phases of head rotation velocity (adjusted  $R^2 = 0.98$ ;  $p < 0.001$ ; Fig. 3B). When both slow and fast phases of head rotation velocity were included (and temporally corrected for a cross-correlation lag of  $-20 \pm 2$  ms), horizontal body rotation velocity correlated with the surround more strongly (adjusted  $R^2 = 0.40$ ;  $p < 0.001$ ). Concentric flight velocity corrected for the bird's position relative to the cylinder center followed similar trends and correlated with the surround speed (adjusted  $R^2 = 0.53$ ;  $p < 0.001$ ; Fig. 3D).

Variability among individuals in all three variables (head and body rotation velocity, and concentric flight velocity) as a function of surround speed was consistently less than the variability observed within individuals (Fig. 3B-D; Table 1).

After stimulus onset, a latency of 52 to 62 ms was observed before the head began tracking the motion of the surround. This latency was conservatively estimated from the instant when mean head orientation exceeded 1 SD (52 ms) of steady head orientation to the instant when the mean exceeded 2 SD (62 ms; Fig. 4).

## Discussion

When presented with a virtually rotating cylindrical surround to induce optic flow, freely flying hummingbirds respond by rotating and flying with the surround (video S1; Fig 2; Fig. 3B-D). Because a perturbation that rotates the bird to the left induces optic flow to the right, the response of tracking the surround with body and head rotations and following the surround with translational flight functionally serves to counter the perturbation caused by the visual presentation. Because the visual presentations do not result in vestibular sensations, this finding strongly indicates that hummingbirds rely on visual cues derived from motion of their surround to stabilize hovering flight.

The hummingbirds consistently and closely matched the imposed rotational speed and flew with the rotating surround, despite the differing spatial and temporal frequencies that varied depending on the birds' positions within the cylinder when presented with the rotating visual stimulus (Fig. 2; 3B-D). The tracking and following responses were robust, as illustrated by an additional 5 s trial, filmed at a lower frame rate, during which the bird responded for more than two full revolutions, partially flying backwards, and only reverted to normal hovering after the stimulus stopped (Video S2). These findings indicate that under free-flight conditions hummingbirds compensate for both rotational and translational optic flow components. Therefore, both components likely serve to control and stabilize flight maneuvers.

Previous findings that flight position in hummingbirds is controlled by optic flow (Goller & Altshuler, 2014) and that hawkmoths stabilize their flight position visually and possess visual interneurons sensitive to translational optic flow (Kern, R. and Varju, D. 1998; Kern, 1998) corroborate our findings. However, our data cannot exclude the possibility that edge fixation on the retina, based on a vertical bar of the virtual surround employed in our experiments, may provide a second possible visual mechanism to control position.

Even though the accuracy (measured as tracking gain; Table 1) and variability (Fig. 3B, C) of the hummingbirds' responses to the imposed wide-field motion of a square-wave grating differed between head rotations and body rotations, head and body tracking of the surround was robust (see, for example, Video S2). During slow rotation phases, the head tracked the surround more accurately (tracking gain = 1.00) compared to the body (tracking gain = 1.48), with perfect tracking signified by a gain of one (measured velocity / imposed velocity). This over-rotation of



the body relative to the surround likely reflects the tendencies of head saccades to be directed with the surround and of the body to follow the head (Fig. 1). This tendency of the head to saccade with the stimulus motion, and thus against the perceived perturbation, is a distinguishing feature compared to the classical optomotor response, where the saccades ('flick back') are predominantly against the stimulus motion (see Turke *et al.*, 1996). Notably, because birds tend to enhance gaze stabilization periods through brief, small eye motions relative to the head (Gioanni, 1988), the hummingbirds' eyes can be expected to track movement of the surround with even higher fidelity than the head. However, because the degree of eye movements relative to the head during flight in hummingbirds is unknown, we could not estimate the discrepancy between head movement and gaze.

The greater variability in tracking of the surround by body rotations than by slow phases of head rotations (Table 1; Fig. 3B, C) likely has multiple causes. First, body rotations are not saccadic in nature, especially when compared to head rotations (Fig. 1 C-E). Consequently, the tendency of the body to follow the head saccades will increase variability in tracking the surround. Second, direct action of neck muscles provides greater control of head movement, whereas movements of the much larger body depend on aerodynamic forces generated by the wings. Body rotations, as observed here, are also likely needed to change flight velocity in order to follow the surround (Ros *et al.*, 2011), in addition to tracking the surround through head and body rotations. Lastly, brief spontaneous maneuvers are characteristic of normal hummingbird behavior (Greenewalt, 1960), and may result in a superposition of normal hovering body rotations on top of the corrective body rotations tracking the surround. Therefore, more variable body stabilization compared to the head can be expected relative to the rotating surround used here to elicit visual perturbations.

We base our conclusions regarding optic flow and flight stabilization on the flight behavior of the hummingbirds as they tracked and followed the surround (Fig. 3). Interpreting underlying components of the observed ~0.5 s latency between the stimulus onset and the birds' stabilized response to rotate and fly with the surround would require knowledge of eye motion and perceptual focus, which are challenging to achieve during free-flight and generally unknown for birds (Fig. 3A; see Gioanni, 1988). We can, however, estimate the delay between stimulus onset and the *initiation* of head rotations to be 52 to 62 ms (Fig 4). The eyes likely respond

earlier than the measured head movements (Gioanni, 1988). Nevertheless, such a delay is longer than visuomotor delays observed in insects (~20 ms, *e.g.*, (Collet & Land, 1975)), consistent with the smaller size and higher wingbeat frequencies of insects (Healy *et al.*, 2013).

In conclusion, as experts in precise and highly maneuverable flight (Lee et al, 1991), freely flying hummingbirds appear to use similar sensory mechanisms to stabilize flight as insects. Our findings corroborate recent findings that Anna's hummingbirds control hovering position in response to projected visual motion (Goller and Altshuler, 2014). Our currently reported visual control of horizontal rotation and flight position in ruby-throated hummingbirds further supports the general view that birds and insects rely on both rotational and translational optic flow components to control flight maneuvers. This suggests convergent evolution on similar principles for robust visually guided flight performance in both groups of flying animals.

## **Acknowledgements**

We thank P. A. Ramirez for care of the animals, and are grateful to Y. Hong, A. N. Ahn, A. M. Mountcastle, C. D. Williams and S. Ravi for helpful contributions. This study was funded by grants from NSF (IOS-0744056) and ONR (N0014-10-1-0951) to AAB.

## References

1. Baird, E., Srinivasan, M. V., Zhang, S. & Cowling, A. 2005. Visual control of flight speed in honeybees. *J. Exp. Biol.* **208**, 3895–3905.
2. Benson, A.J. 1990. Sensory functions and limitations of the vestibular system. In *Perception and control of self-motion*. Warren R. & Wertheim A. H. (Eds). Erlbaum, Hillsdale, NJ, USA.
3. Bhagavatula, P. S., Claudianos, C., Ibbotson, M. R., Srinivasan, M. V. 2011. Optic Flow Cues Guide Flight in Birds. *Curr. Biol.* **21**, 1794-1799.
4. Bilo, D. 1992. Optocollic reflexes and neck flexion-related activity of flight control muscles in the airflow-stimulated pigeon. In: Berthoz A, Graf W, Vidal PP (Eds). *The head-neck sensory motor system*. Oxford University Press: Oxford.
5. Collett, T. S. and Land, M. F. 1975. Visual control of flight behaviour in the hoverfly, *Syritta pipiens* L. *J. Comp. Physiol.* **99**, 1-65.
6. Crowder N. A., Dawson M. R. and Wylie D. R. 2003. Temporal frequency and velocity-like tuning in the pigeon accessory optic system. *J Neurophysiol* **90**: 1829-1841.
7. Davies, M. N. O. & Green, P. R. 1990. Optic flow-field variable trigger landing in hawk but not in pigeons. *Naturwissenschaften* **77**, 142-144.
8. Dudley, R. 2002 Mechanisms and implications of animal flight maneuverability. *Integr. Comp. Biol.* **42**, 135 -140.
9. Dudley, R. 2002. *The Biomechanics of Insect Flight: Form, Function, Evolution*. Princeton Univ Press, Princeton, NJ, USA.
10. Eckmeier, D., Geurten, B. R. H., Kress, D., Mertes, M., Kern, R., Egelhaaf, M., Bischof, H. J. 2008. Gaze strategy in the free flying zebra finch (*Taeniopygia guttata*). *PLOS ONE* **3**, e3956.
11. Eckmeier, D., Kern, R., Egelhaaf, M., & Bischof, H. J. 2013. Encoding of naturalistic optic flow by motion sensitive neurons of nucleus rotundus in the zebra finch (*Taeniopygia guttata*). *Front. Integr. Neurosci.* **7**.
12. Egelhaaf, M., Hausen, K., Reichardt, W., and Wehrhahn, C. 1988. Visual course control in flies relies on neuronal computation of object and background motion. *Trends in Neurosc.* **11**, 351-358.

13. Egelhaaf, M., Boeddeker, N., Kern, R., Kurtz, R., and Lindemann, J. P. 2012. Spatial vision in insects is facilitated by shaping the dynamics of visual input through behavioral action. *Front. Neur. Circ.* **6**, 108.
14. Farina WM, Kramer D, Varju D. 1995 The response of the hovering hawk moth *Macroglossum stellatarum* to translatory pattern motion. *J. Comp. Physiol. A* **176**, 551–562.
15. Fry, S. N., Rohrseitz, N., Straw A. D., and Dickinson, M.H. 2009. Visual control of flight speed in *Drosophila melanogaster*. *J. Exp. Biol.* **212**, 1120–1130.
16. Friedman, M. B. 1975. Visual control of head movements during avian locomotion. *Nature* **255**, 67–69.
17. Gewecke, M. and Woike, M. 1978. Breast feathers as an air-current sense organ for the control of flight behaviour in a songbird (*Carduelis spinus*). *Z. Tierpsychol.* **47**, 293–298.
18. Gibson, J. J. 1958. Visually controlled locomotion and visual orientation in animals. *Brit. J. Psychol.* **49**, 182-194.
19. Gioanni, H. 1988. Stabilizing gaze reflexes in the pigeon (*Columba livia*). I. Horizontal and vertical optokinetic eye (OKN) and head (OCR) reflexes. *Exp. Brain Res.* **69**, 567–582.
20. Gioanni, H. and Sansonetti, A. 1999. Characteristics of slow and fast phases of the optocollic reflex (OCR) in head free pigeons (*Columba livia*): influence of flight behaviour. *Eur. J. Neurosci.* **11**, 155-166.
21. Goller, B., and Altshuler, D. L. 2014. Hummingbirds control hovering flight by stabilizing visual motion. *PNAS*, **111**, 18375-18380.
22. Greenewalt C. H. 1960. *Hummingbirds*. Doubleday: New York, NY, USA.
23. Guckenheimer, J. and Holmes P. 2013. Nonlinear oscillations, dynamical systems, and bifurcations of vector fields. Springer, Berlin, Germany.
24. Healy, K., McNally, L., Ruxton, G. D., Cooper, N., & Jackson, A. L. 2013. Metabolic rate and body size are linked with perception of temporal information. *Anim. Behav.* **86**, 685-696.
25. Hedrick, T. L. 2008. Software techniques for two- and three-dimensional kinematic measurements of biological and biomimetic systems. *Bioinspir. Biomim.* **3**, 034001.

26. Ibbotson, M. R., and Price, N. S. 2001. Spatiotemporal tuning of directional neurons in mammalian and avian pretectum: a comparison of physiological properties. *J. Neurophys.* **86**, 2621-2624.
27. Iwaniuk A. N. and Wylie D. R. 2007. Neural specialization for hovering in hummingbirds: Hypertrophy of the pretectal nucleus lentiformis mesencephali. *J. Comp. Neur.* 500: 211-221.
28. Kern, R. and Varju, D. 1998. Visual position stabilization in the hummingbird hawk moth, *Macroglossum stellatarum* L. I. Behavioural analysis. *J. Comp. Physiol. A Neuroethol. Sens. Neural Behav. Physiol.* **182**, 225–237.
29. Kern, R. 1998. Visual position stabilization in the hummingbird hawk moth, *Macroglossum stellatarum* L. II. Electrophysiological analysis of neurons sensitive to wide-field image motion. *J. Comp. Physiol. A Neuroethol. Sens. Neural Behav. Physiol.* **182**, 239-249.
30. Koenderink, J. J. 1986. Optic flow. *Vis. Res.* **26**: 161–179.
31. Koenderink, J. J., and Van Doorn, A. J. 1987. Facts on optic flow. *Biol. Cybern.*, **56**, 247-254.
32. Lee, D. N., Davies, M. N. O., Green, P. R., Van Der Weel, F. R. R. 1993. Visual control of velocity of approach by pigeons when landing. *J. Exp. Biol.* **180**, 85-104.
33. Lee, D. N., Reddish, P. E., Rand, D. T. 1991. Aerial docking by hummingbirds. *Naturwissenschaften* **78**, 526-527.
34. Mronz, M., and Lehmann, F. O. 2008. The free-flight response of *Drosophila* to motion of the visual environment. *J. Exp. Bio.* **211**, 2026-2045.
35. Nakayama K. 1981. Differential motion hyperacuity under conditions of common image motion. *Vis. Res.* **21**, 1475-1482.
36. Reichardt, W. 1969. Movement perception in insects. In: Reichardt, W. (Ed) Processing of optical data by organisms and insects. Academic Press, New York, pp 465-493.
37. Ros, I. G., Bassman, L. C., Badger, M. A., Pierson, A. N., Biewener, A. A. 2011. Pigeons steer like helicopters and generate down- and upstroke lift during low speed turns. *PNAS* **108**, 19990-19995.
38. Sefati, S. *et al.* 2013. Mutually opposing forces during locomotion can eliminate the tradeoff between maneuverability and stability. *PNAS*, **110**, 18798-18803.

39. Schiffner, I., and Srinivasan, M. V. 2015. Direct Evidence for Vision-based Control of Flight Speed in Budgerigars. *Scientific reports*, **5**.
40. Simpson, J. I. 1984. The accessory optic system. *Annu. Rev. Neurosci.* **7**, 13–41.
41. Srinivasan, M. V. 2001. Visual navigation: the eyes know where their owner is going. In *Motion Vision – Computational, Neuronal, and Ecological Constraints* (eds. J. M. Zanker & J. Zeil) (Springer: Berlin, Germany).
42. Srinivasan, M., Zhang, S., Lehrer, M. and Collett, T. 1996. Honeybee navigation en route to the goal: visual flight control and odometry. *J. Exp. Biol.* **199**, 237–244.
43. Theobald, J. C., Warrant, E. J., and O'Carroll, D. C. 2009. Wide-field motion tuning in nocturnal hawkmoths. PRSB, rspb20091677.
44. Türke, W., Nalbach, H. O., and Kirshfeld, K. 1996. Visually elicited head rotation in pigeons (*Columba livia*). *Vis. Res.* **36**, 3329-3337.
45. Walls G. L. 1962. The evolutionary history of eye movements. *Vis. Res.* **2**, 69-80.
46. Westheimer, G., and McKee, S. P. 1975. Visual acuity in the presence of retinal-image motion. *J.O.S.A.* **65**, 847-850.
47. Windsor, S. P., Bomphrey, R. J., and Taylor, G. K. 2014. Vision-based flight control in the hawkmoth *Hyles lineata*. *JRSI.* **11**, 20130921.
48. Wylie D. R. and Frost B. J. 1990. Binocular neurons in the nucleus of the basal optic root (nBOR) of the pigeon are selective for either translational or rotational visual flow. *Vis Neurosci* **5**: 489–495.

## Figures

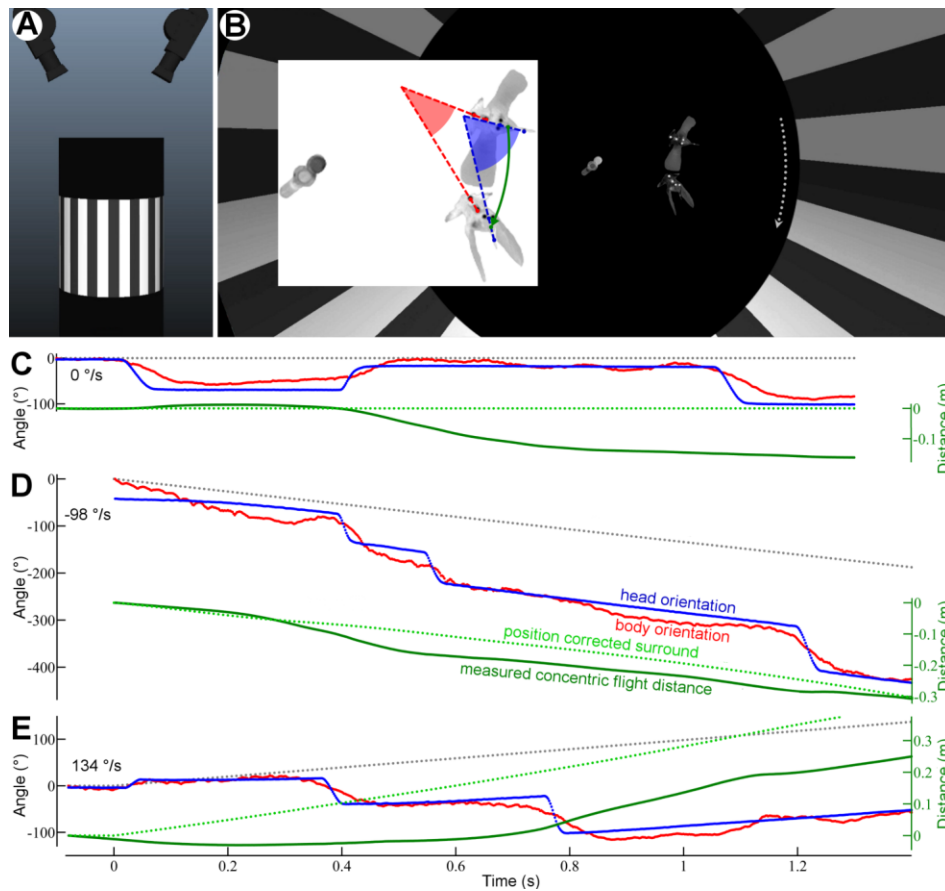


**Figure 1. Free-flying hummingbirds track and follow surround rotations, likely reducing optic flow.** (A, B) High-speed video cameras (black silhouettes) record hummingbirds flying freely within a vertical, hollow, 1.2m-diameter cylinder. (B) Top view. A hummingbird, depicted twice, 0.02 s apart, moves clockwise (cw) with the rotating surround (dotted grey arrow). A feeder is suspended vertically at the cylinder center. Inset (greyscale inverted for clarity): body orientation (red shaded triangle), head orientation (blue shaded triangle) and concentric flight distance (green), all within the horizontal. (C-E) Representative trials at surround speeds of  $0^{\circ} \text{ s}^{-1}$  (C),  $-98^{\circ} \text{ s}^{-1}$  (ccw) (D), and  $134^{\circ} \text{ (cw) s}^{-1}$  (E) (dotted grey traces), with the surround projected at 120 frames per second. Body and head orientation are referenced against the body orientation at rotation onset (time = 0 s), with flight distance measured from the initial measurement



position. To follow the wall, the hummingbird must fly concentrically at speeds depending on its distance from the cylinder center and the imposed surround velocity. The concentric flight speed integrated over time that is required to compensate for wide-field motion is the position-corrected surround distance (green dotted trace, green axes).

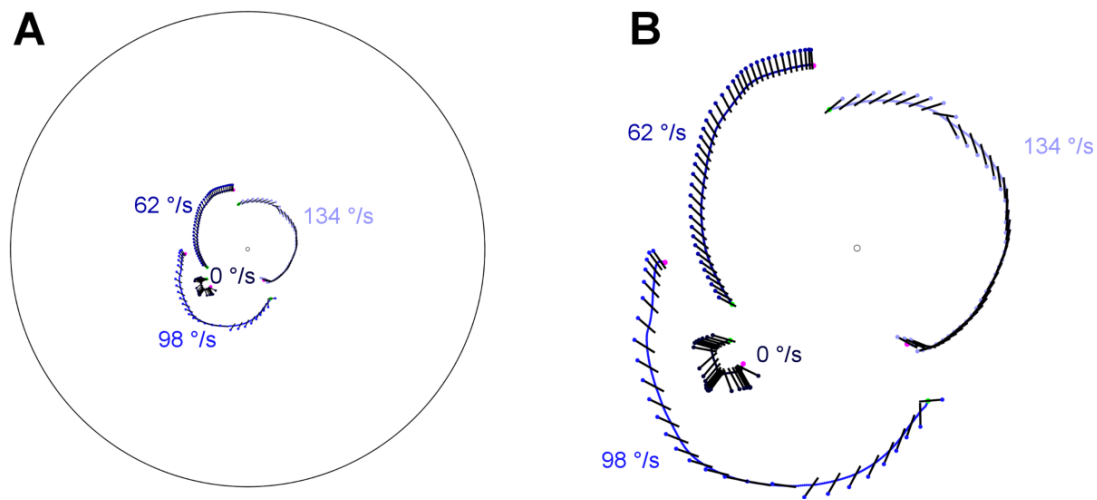


**Figure 2. Projected surround rotations result in a tracking and following behavior.** (A) Top view of the cylinder (to scale), with flight path (blue-shade traces) and head orientation (short black lines with blue-shade circle at the bill tip) represented once per wingbeat cycle. Representative trials illustrating the tracking and following behavior for flights from 0.5 s (green dots) to 1.5 s (magenta dots) after clockwise stimulus rotation onset, for 62, 98 and 134 ° s<sup>-1</sup>, and for a non-rotating surround (0 ° s<sup>-1</sup>). (B) Enlarged view of the traces in (A) around the feeder at the cylinder center (small black circle).

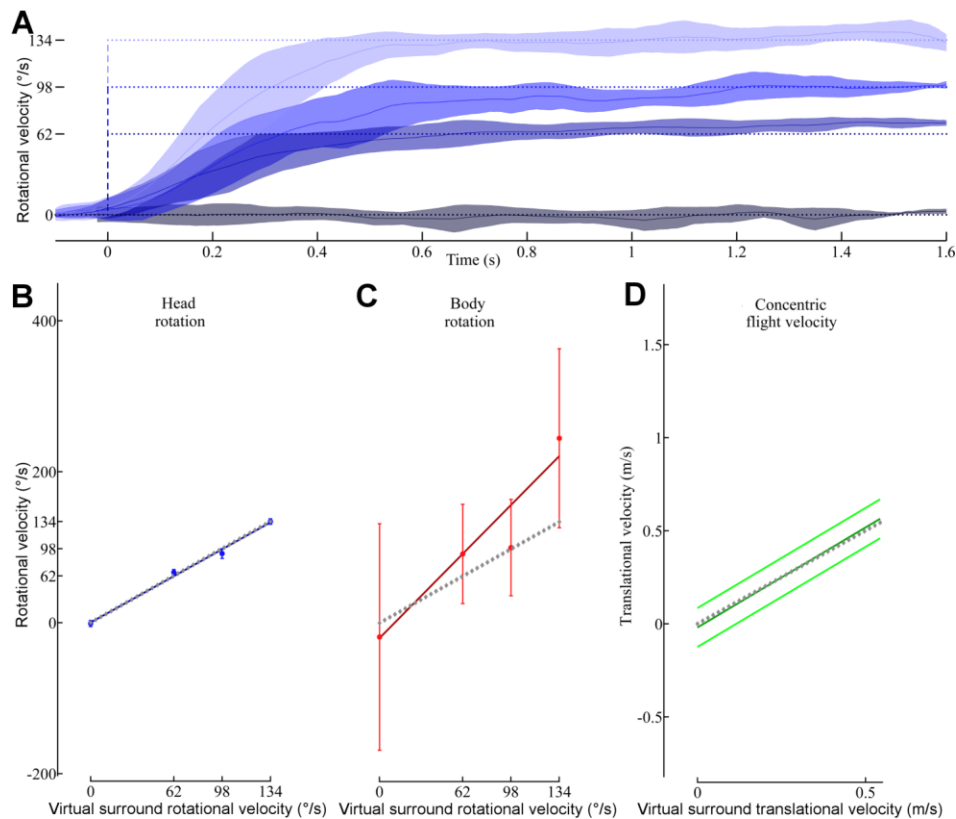


**Figure 3. Rotational velocities of the head and body, and translational flight velocities match projected surround speeds.** (A) Head rotation velocity, averaged across individuals (solid traces  $\pm$  shading (SD)), begins matching imposed surround speed (dotted traces) approximately 0.5 seconds following stimulus onset ( $t = 0$  s), for all three surround speeds. Note that fast phases (head saccades) are omitted to illustrate tracking during the slow phases. (B-D) Between 0.5 s to 1.5 s after stimulus onset, head (blue) and body (red) rotation velocities and concentric flight velocities (green) correlate with corresponding surround velocities (solid dark prediction lines;  $p < 0.001$  for all three variables), although variation in body rotation tracking (c) is considerably greater than head rotation tracking (B) of the surround. Means  $\pm$  SD (error bars in b, c; light green traces in d) illustrate surround tracking (B, C) and following (D) (grey dashed lines).

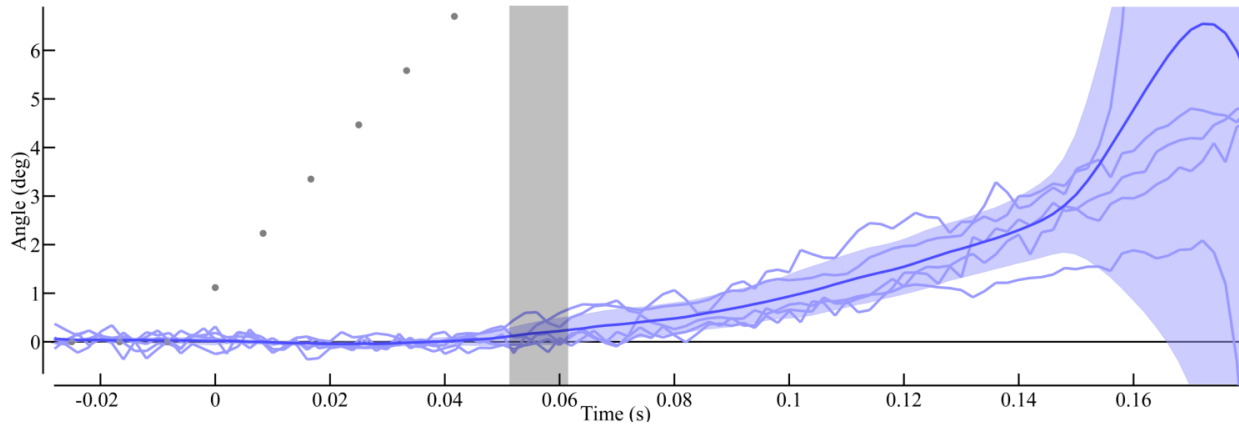


**Figure 4. Hummingbirds start tracking the surround within 62 ms.** Unfiltered head orientations of five individuals for a surround speed of  $134^{\circ} \text{ s}^{-1}$  (light blue lines), as well as the mean  $\pm$  SD (dark blue trace and shaded area), with the visuo-mechanical delay conservatively estimated between 52-62 ms (grey shading).

**Table 1.** Measured velocities are directed with the surround (+).

tracking gain (measured/surround) across individuals (N=5)	between individuals (mean $\pm$ SD)	within individuals (mean SD)
head rotation velocity (slow phases)	1.01 $\pm$ 0.04	0.10
body rotation velocity	1.48 $\pm$ 0.68	2.32
concentric flight velocity	0.93 $\pm$ 0.22	0.66



**Movie 1. Visualization of the experimental setup.** A female hummingbird, with the five markers visible, hovers within the cylinder near the centrally suspended feeder. The high speed camera positioning and the projected virtual surround are emphasized at the start of the video. The bird can be seen rotating both head and body, and flying with the virtually rotating surround.



**Movie 2. A hummingbird tracking and following the virtual surround.** The bars projected on the cylinder wall move clockwise at  $134^\circ \text{ s}^{-1}$ . The high-speed video, recorded as an additional trial, has been down-sampled to play at approximately one-third of the real speed. Note at the end that the bird ceases to rotate its head and body, and ceases to fly concentrically when the projected rotation is arrested.